Polymer Chemistry

Cite this: *Polym. Chem.*, 2012, **3**, 2112

www.rsc.org/polymers

PAPER

Fluorinated polyhedral oligomeric silsesquioxane-based shape amphiphiles: molecular design, topological variation, and facile synthesis†

Jinlin He,‡[ab] Kan Yue,‡[a] Yuqing Liu,[a] Xinfei Yu,[a] Peihong Ni,[b] Kevin A. Cavicchi,[a] Roderic P. Quirk,[a] Er-Qiang Chen,*[c] Stephen Z. D. Cheng*[a] and Wen-Bin Zhang*[a]

Received 24th February 2012, Accepted 18th April 2012
DOI: 10.1039/c2py20101a

This paper reports the design and synthesis of fluoroalkyl-functionalized polyhedral oligomeric silsesquioxane (FPOSS)-based shape amphiphiles with two distinct topologies: (i) mono-tethered FPOSS-poly(ε-caprolactone) (PCL) and (ii) FPOSS tethered with two polymer chains possessing different compositions, namely, polystyrene (PS) and PCL, denoted as PS–(FPOSS)–PCL. The synthetic strategy features an efficient "growing-from" and "click-functionalization" approach. From a monohydroxyl-functionalized heptavinyl POSS, a PCL chain was grown *via* ring opening polymerization (ROP) of ε-caprolactone; subsequent thiol–ene "click" chemistry with 1*H*,1*H*,2*H*,2*H*-perfluoro-1-decanethiol allowed the facile introduction of seven perfluorinated alkyl chains onto the POSS head. Similarly, PS–(FPOSS)–PCL was synthesized from a PS precursor bearing both hydroxyl group and heptavinyl POSS at the ω-end, which was prepared by living anionic polymerization and hydrosilylation. The compounds were fully characterized by ^{1}H NMR, ^{13}C NMR, FT-IR spectroscopy, MALDI-TOF mass spectrometry, and size exclusion chromatography. The introduction of perfluorinated molecular cluster into polymers is expected to make them surface-active while the interplay between crystallization and fluorophobic/fluorophilic bulk phase separation in these shape amphiphiles shall lead to intriguing self-assembly behavior and novel hierarchical structures. This study has demonstrated FPOSS as a versatile building block in the construction of shape amphiphiles and established a general and efficient method to introduce such fluorous molecular clusters into polymers.

Introduction

Shape amphiphiles refer to the fusion of molecular building blocks with both incommensurate shapes and competing interactions.[1–3] While rigid shapes often impose considerable packing constraints, the amphiphilic interactions between shaped objects are the primary driving force for their self-assembly. Such interactions often arise from the presence of multiple functional groups on the surface/periphery of a particular shaped object, leading to rich phase behaviors and novel hierarchical structures as shown by recent computer simulations.[2–5] They have thus emerged as a novel approach for the controlled, rational creation of functional structures in multiple length scales. Typical shape amphiphiles are composed of a nano-building block tethered with one or more polymer chains at specific locations.[4–7] A large number of nano-building blocks with distinct geometry/symmetry (nanospheres, nanoplates, nanocubes, nanotetrapods, *etc.*),[8,9] chemical composition (inorganic or organic),[10,11] and surface chemistry (hydrophilic, hydrophobic, or fluorophilic)[6,7] have been developed over the past decades with the booming of nano-science and technology.[3,12] They include inorganic metal clusters and nano-crystals,[13] dendrimers,[14] polymers,[15] and molecular nanoparticles (MNPs), among which polyhedral oligomeric silsesquioxanes (POSS)[16] and fullerene (C_{60})[17] have attracted enormous research interest as a result of well-defined structure and chemical modification. Recently, we have utilized both POSS and C_{60} as versatile building blocks to develop shape amphiphiles with precise control of molecular parameters such as chemical compositions, overall size/shape, and locations of functionalities.[6,7,18–20] It has also been shown that such shape amphiphiles are quite versatile in self-assembly and behave like small-molecule surfactants and diblock copolymers in certain aspects.[6] As part of our efforts towards a systematic

[a]*College of Polymer Science and Polymer Engineering, The University of Akron, Akron, OH, 44325-3909, USA. E-mail: wz8@uakron.edu; scheng@uakron.edu; Fax: +1 330 972 8626; Tel: +1 330 972 6931; +1 330 990 9801*
[b]*College of Chemistry, Chemical Engineering, and Materials Science, Jiangsu Key Laboratory of Advanced Functional Polymer Design and Application, Soochow University, Suzhou 215123, P. R. China*
[c]*Department of Polymer Science and Engineering and Key Laboratory of Polymer Chemistry and Physics of Ministry of Education, College of Chemistry and Molecular Engineering, Peking University, Beijing 100871, P. R. China. E-mail: eqchen@pku.edu.cn; Fax: +86 10 62753370; Tel: +86 10 62753370*

† Electronic supplementary information (ESI) available. See DOI: 10.1039/c2py20101a

‡ These authors contributed equally to this work.

understanding of their structure–property relationships, we aim to develop synthetic strategies for fine-tuning of relevant molecular parameters: (1) surface chemistry on the MNPs, (2) chain topology and (3) chain composition of the tethered polymer chains. While variance in chain topology and composition has been shown in fullerene polymers, the diversity of surface chemistry on MNPs has been largely limited to hydrophilic/hydrophobic interactions so far. To further expand the scope and utility of shape amphiphiles, it is of great interest to introduce the fluorous interaction into the system.

The fluorous phase[21] is considered to be the third phase beyond the aqueous and oil phases – it does not mix with most common organic solvents or aqueous solvents at room temperature. Due to their unique features such as relatively high density, low surface energy, extreme chemical inertness, and excellent thermal stability, the fluorinated compounds have received intense research interest in materials science and found numerous practical applications.[22] Various hybrid fluorous materials have been developed, among which the fluorous molecular clusters (such as highly fluorinated C_{60} and POSS) are of particular interest.[23,24] Not only could they be used as lubricants and superhydrophobic additives, but they are also versatile building blocks for further chemical modification into functional hybrid materials. The preparation of such highly fluorinated nano-particles involves either direct fluorination or attaching multiple "ponytails" with the general formula of $-(CH_2)_m(CF_2)_{n-1}CF_3$ to the particle. For example, fluorinated POSS (FPOSS) have been prepared both by direct condensation of perfluorinated siloxanes[23] and by attaching "ponytails" to an organic-soluble vinyl POSS precursor *via* thiol–ene chemistry in a single step.[18] Due to the high incompatibility between fluorous chain molecular segments and common organic molecules, the latter approach is perhaps more advantageous in generating well-defined structures, especially in combination with "click" chemistry and other efficient chemical transformations, such as Cu(I)-catalyzed [3 + 2] azide–alkyne cycloaddition (CuAAC)[25,26] and thiol–ene reaction,[27,28] for peripheral, simultaneous multiple-site functionalization. A thus-formed FPOSS MNP is a porcupine-like molecular cluster with a diameter of several nanometres and is expected to be strongly phase-separated from the rest of the molecule. This unique 3D structure makes it highly attractive as a fluorous nano-building block.

In this paper, we report the use of FPOSS as a building block in shape amphiphiles with different topologies and compositions and demonstrate post-functionalization by thiol–ene "click" chemistry as a general and efficient method for their synthesis. Two different types of shape amphiphiles were designed and synthesized. The FPOSS-end capped poly(ε-caprolactone) (FPOSS-PCL) was prepared in two steps from a simple precursor, monohydroxyl-functionalized heptavinyl POSS (VPOSS–OH), following a "growing-from" and "post-functionalization" strategy (Scheme 1).[7] Similarly, a FPOSS tethered with polystyrene (PS) and PCL chains at the junction point, PS–(FPOSS)–PCL, was synthesized from a PS macroinitiator bearing both hydroxyl group and heptavinyl POSS at the ω-end (Scheme 2).[6,7] These shape amphiphiles with fluorous head group and distinct tethered chain topology and composition are important novel compounds for the study of their physics and self-assembled structures.

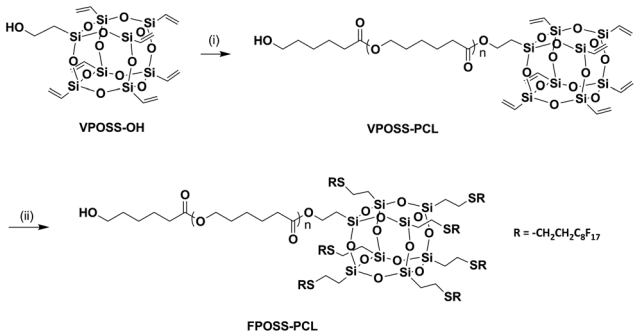

Scheme 1 Synthesis of FPOSS–PCL: (i) $Sn(Oct)_2$, ε-CL, toluene, 65 °C, 54%; (ii) $C_8F_{17}CH_2CH_2SH$, DMPA, $CHCl_3$, *hv*, 15 min, 72%.

Experimental section

Chemicals and solvents

sec-Butyllithium (FMC Lithium, 12 wt% in cyclohexane) was used after double titration with allyl bromide.[29] Benzene (EMD, ACS grade), toluene (EMD, ACS grade), ethylene oxide (99.5+%, Aldrich), and styrene (99%, Aldrich) were purified as previously reported for anionic polymerizations.[30] Methanol (Fisher Scientific, Certified ACS) was degassed on the vacuum line before distillation into ampoules and flame-sealed. Other solvents, such as chloroform (Fisher Scientific, Certified ACS), hexanes (Fisher Scientific, Certified ACS), tetrahydrofuran (THF, EMD, ACS grade) were used as received. ε-Caprolactone (ε-CL, 99%, Acros) was dried over calcium hydride for 24 hours at room temperature and distilled under reduced pressure before use. Tin(II) 2-ethylhexanoate [$Sn(Oct)_2$, Aldrich, 95%] was fractionally distilled and diluted with anhydrous degassed toluene to make a 1.0 M solution before use. OctaVinyl-POSS (OVPOSS, >97%, Hybrid Plastics), Karstedt's catalyst, 1,3-divinyltetramethyl-disiloxaneplatinum (Gelest, 1.2–1.4 wt% Pt in xylene), 2,2-dimethoxy-2-phenylacetophenone (DMPA, 99%, Acros),

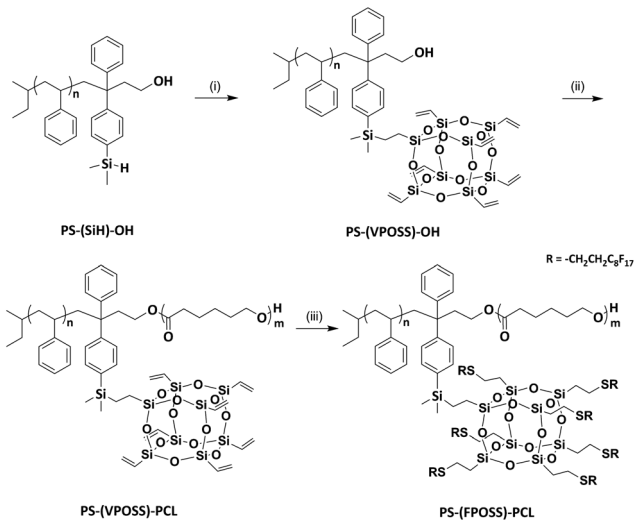

Scheme 2 Synthesis of PS–(FPOSS)–PCL: (i) OVPOSS, Karstedt's catalyst, toluene, r.t., 44%; (ii) $Sn(Oct)_2$, ε-CL, toluene, 65 °C, 59%; (iii) $C_8F_{17}CH_2CH_2SH$, DMPA, $CHCl_3$, *hv*, 15 min, 75%.

1*H*,1*H*,2*H*,2*H*-perfluoro-1-decanethiol (97%, Aldrich), trifluoromethanesulfonic acid (ReagentPlus®, >99%, Aldrich), and *N*,*N*-dimethylformamide (anhydrous, 99.8%, Aldrich) were used as received. Silica gel (Sorbtech Technologies, 230–400 mesh) was activated by heating to 140 °C for 12 hours. VPOSS–OH was prepared from OVPOSS according to the literature procedure.[31] Dimethyl-[4-(1-phenylvinyl)phenyl]silane (DPE-SiH) and PS–(SiH)–OH ($M_{n,SEC}$ = 6.9 kg mol^{-1}, M_w/M_n = 1.02) were synthesized as reported in our previous work.[32]

Instrumentation and characterization

Size exclusion chromatographic (SEC) analyses for the XPOSS-PCL series were performed using a Waters Breeze system with three Styragel columns at 35 °C and a refractive index detector. Samples were run at a flow rate of 0.5 mL min^{-1} with THF as the mobile phase. For the PS–(XPOSS)–PCL series, SEC analyses were performed on a Waters 150-C Plus instrument equipped with three HR-Styragel columns [100 Å, mixed bed (50/500/10^3/10^4 Å), mixed bed (10^3, 10^4, 10^6 Å)], and a triple detector system. The three detectors included a differential refractometer (Waters 410), a differential viscometer (Viscotek 100), and a laser light scattering detector (Wyatt Technology, DAWN EOS, λ = 670 nm). THF was used as eluent with a flow rate of 1.0 mL min^{-1} at room temperature. The molecular weight *vs.* elution time was calibrated using narrow polydispersed polystyrene standards.

All ^{1}H and ^{13}C nuclear magnetic resonance (NMR) spectra were obtained in $CDCl_3$ (Aldrich, 99.8% D) as solvent using a Varian Mercury 500 NMR spectrometer. The ^{1}H NMR spectra were referenced to the residual proton impurities in the $CDCl_3$ at δ 7.27 ppm. ^{13}C NMR spectra were referenced to $^{13}CDCl_3$ at δ 77.00 ppm.

Infrared spectra were recorded on an Excalibur Series FT-IR spectrometer (DIGILAB, Randolph, MA) by casting polymer films on KBr plates from polymer solutions (about 10 mg mL^{-1}) with subsequent drying by blowing with air. The data were processed using Win-IR software.

Matrix-assisted laser desorption/ionization time-of-flight (MALDI-TOF) mass spectra were recorded on a Bruker Ultraflex III TOF/TOF mass spectrometer (Bruker Daltonics, Billerica, MA), which was equipped with a Nd : YAG laser emitting at a wavelength of 355 nm. *trans*-2-[3-(4-*tert*-Butylphenyl)-2-methyl-2-propenylidene]malononitrile (DCTB, Aldrich, >99%) served as matrix and was prepared in $CHCl_3$ at a concentration of 20.0 mg mL^{-1}. The polymer sample was dissolved in $CHCl_3$ at 5 mg mL^{-1}. Sodium trifluoroacetate (NaTFA) and lithium trifluoroacetate (LiTFA) served as cationizing agents and were prepared in MeOH–$CHCl_3$ (1/3, v/v) at a concentration of 10 mg mL^{-1}. The matrix and cationizing agent were mixed in the ratio of 10/1 (v/v). The sample preparation involved depositing 0.5 μL of the mixture of matrix and salt on the wells of a 384-well ground-steel plate, allowing the spots to dry, depositing 0.5 μL of each sample on a spot of dry matrix, and adding another 0.5 μL of the mixture of matrix and salt on top of the dry sample (the sandwich method).[33] Mass spectra were measured in the reflectron mode, and the mass scale was calibrated externally using the peaks obtained from a polystyrene or PMMA standard at the molecular weight range under consideration. Data analyses were conducted with Bruker's flex Analysis software.

Molecular weight calculation was based on the peak area integration ratio in ^{1}H NMR spectra between the peaks at δ ~4.07 ppm (–CH_2O– in PCL) or the peaks at δ 7.40–6.32 ppm (aromatic protons in PS) and the characteristic peaks at the POSS cage (21H at δ 6.15–5.88 ppm for VPOSS–PCL, PS–(VPOSS)–OH, and PS–(VPOSS)–PCL; 28H at δ 2.80–2.60 ppm for FPOSS–PCL and PS–(FPOSS)–PCL) that gives the number average degree of polymerization, *n*, of each polymeric block. The molecular weight can be obtained by the summation of $M_{n,PCL}$ (n × 114.1), $M_{n,PS}$ (n × 104.1) and M_{XPOSS} (650.0 for VPOSS; 4009.8 for FPOSS).

VPOSS–PCL. A Schlenk flask equipped with a magnetic stirrer was connected to a high vacuum line and flame-dried three times. After cooling down to room temperature, VPOSS–OH (70 mg, 0.11 mmol), ε-CL (1.23 g, 10.8 mmol), 10 mL of anhydrous toluene, and $Sn(Oct)_2$ (1.0 M in toluene, 0.054 mL, 0.054 mmol) were added. The mixture was degassed by three freeze–pump–thaw cycles, and placed into an oil bath of 65 °C. After a definite time, the flask was cooled in ice-water. The mixture was then precipitated into cold methanol three times. The resulting white solids were collected after filtration and dried at 25 °C under vacuum overnight to give 0.70 g of VPOSS–PCL as a white powder. Yield: 54%. ^{1}H NMR ($CDCl_3$, 500 Hz, ppm, δ): 6.15–5.88 (m, 21H, -CH=CH_2), 4.01 (m, 118H), 3.58 (t, 2H, -CH_2OH), 2.26 (m, 119H), 1.60 (m, 240H), 1.33 (m, 118H). ^{13}C NMR ($CDCl_3$, 125 Hz, ppm, δ): shown in Fig. S1a†. FT-IR (KBr) ν (cm^{-1}): 3542, 3439, 2945, 2866, 1726 (C=O), 1603, 1469, 1367, 1295, 1243, 1190, 1109, 1047, 962, 733, 586. MS (MALDI-TOF): calcd monoisotopic mass for 32-mer [M_{32}·Na]$^+$ ($C_{208}H_{346}O_{77}Si_8Na$): 4323.1 Da; found: *m*/*z* 4323.3 Da. $M_{n,NMR}$ = 7.4 kg mol^{-1}. SEC: $M_{n,SEC}$ = 8.1 kg mol^{-1}, M_w/M_n = 1.12.

FPOSS–PCL. In an open vial, VPOSS–PCL (100 mg, 13.5 μmol, 1 eq.), 1*H*,1*H*,2*H*,2*H*-perfluoro-1-decanethiol (72 mg, 0.15 mmol, 11 eq. per polymer or 1.6 eq. per vinyl), and DMPA (1.0 mg, 3.9 μmol) were mixed and dissolved in 1.5 mL of $CHCl_3$. After irradiation with UV 365 nm for 15 min, the mixture was purified by repeated precipitations in cold methanol–hexanes (v/v = 10/1) to give a white powder (102 mg). Yield: 72%. ^{1}H NMR ($CDCl_3$, 500 Hz, ppm, δ): 4.03 (m, 118H), 3.61 (t, 2H, -CH_2OH), 2.72–2.63 (m, 28H), 2.35–2.26 (m, 128H), 1.64–1.55 (m, 248H), 1.37–1.32 (m, 126H). ^{13}C NMR ($CDCl_3$, 125 Hz, ppm, δ): shown in Fig. S1b†. FT-IR (KBr) ν (cm^{-1}): 3537, 3439, 2945, 2866, 1725 (C=O), 1469, 1367, 1241, 1195, 1152, 1110, 1046, 962, 733, 705, 652. MS (MALDI-TOF): calcd mass for 32-mer [M_{32}·Na]$^+$ ($C_{278}H_{381}F_{119}O_{77}S_7Si_8Na$): 7686.0 Da (100%); found: *m*/*z* 7683.8 Da (100%). $M_{n,NMR}$ = 10.7 kg mol^{-1}. SEC: M_n = 9.6 kg mol^{-1}, M_w/M_n = 1.10.

PS–(VPOSS)–OH. In a vial, four drops of Karstedt's catalyst was added to a mixture of PS–(SiH)–OH ($M_{n,SEC}$ = 6.9 kg mol^{-1}, 0.50 g, 0.073 mmol), OVPOSS (69 mg, 0.109 mmol), and dry toluene (~2 mL). The reaction was then stirred at 50 °C and the progress of the reaction was monitored by FT-IR analysis. After the band for the Si–H stretching vibration mode at ~2115 cm^{-1} completely disappeared, the reaction mixture was precipitated in cold methanol (~50 mL). The solid powder was collected and purified by silica gel chromatography using toluene as

solvent (R_f = 0.50–0.55) to afford mono-functionalized PS–(VPOSS)–OH, (0.24 g, 44%) as a white powder. ^{1}H NMR ($CDCl_3$, 500 Hz, ppm, δ): 7.30–6.30 (m, 332H), 6.25–5.78 (m, 21H, -C*H*=CH_2), 2.95 (m, 2H, -CH_2OH), 2.30–1.00 (m, 210H), 1.00–0.55 (m, 10H), 0.35–0.15 (m, 6H). ^{13}C NMR ($CDCl_3$, 125 Hz, ppm, δ): shown in Fig. S3b†. FT-IR (KBr) ν (cm^{-1}): 3060, 3027, 2924, 2853, 1947, 1874, 1806, 1745, 1601, 1493, 1451, 1120 (Si–O–Si), 1069, 909, 758, 700, 543. MS (MALDI-TOF): calcd monoisotopic mass for 55-mer $[M_{55}\cdot Na]^+$ ($C_{478}H_{496}Si_9O_{13}Na$): 6718.6 Da; found: *m*/*z* 6719.5 Da. $M_{n,NMR}$ = 7.6 kg mol^{-1}. SEC: $M_{n,SEC}$ = 7.7 kg mol^{-1}, M_w/M_n = 1.01.

PS-(VPOSS)–PCL. In a dry box, PS–(VPOSS)–OH (90 mg, 0.0117 mmol) and 6 mL of dry toluene were added into a dry Schlenk flask, which was taken out of the dry box and degassed once on the high vacuum line. ε-CL (268 mg, 2.34 mmol) and $Sn(Oct)_2$ (1.0 M in toluene, 0.10 mL, 0.10 mmol) were then added into the reaction flask under the argon flow. The mixture was then degassed on the high vacuum line by two more freeze–pump–thaw cycles and immersed in an oil bath of 65 °C. After 24 h, the flask was cooled in ice-water and the mixture was precipitated into cold methanol. The white powder was collected after filtration and dried at 25 °C in a vacuum oven for 24 h to give PS–(VPOSS)–PCL as a white powder (0.21 g, 59%). ^{1}H NMR ($CDCl_3$, 500 Hz, ppm, δ): 7.30–6.30 (m, 332H), 6.25–5.78 (m, 21H, -C*H*=CH_2), 4.01 (m, 228H), 3.65 (t, 2H, -CH_2OH), 2.36 (m, 234H), 2.10–1.00 (m, 910H), 1.00–0.55 (m, 10H), 0.35–0.15 (m, 6H). ^{13}C NMR ($CDCl_3$, 125 Hz, ppm, δ): shown in Fig. S3c†. FT-IR (KBr) ν (cm^{-1}): 2938, 2865, 1728 (C=O, very strong), 1455, 1366, 1242, 1184, 1106, 756, 700. $M_{n,NMR}$ = 20.6 kg mol^{-1}. SEC: $M_{n,SEC}$ = 12.9 kg mol^{-1}, M_w/M_n = 1.04.

PS–(FPOSS)–PCL. In an open vial, PS–(VPOSS)–PCL (50 mg, 3.88 μmol, 1 eq.), 1*H*,1*H*,2*H*,2*H*-perfluoro-1-decanethiol (20.5 mg, 43 μmol, 11 eq. per polymer or 1.6 eq. per vinyl) and DMPA (0.5 mg, 1.95 μmol, 0.5 eq. per polymer or 7 mol% per vinyl) were mixed and dissolved in ~2 mL of $CHCl_3$. After irradiation with UV 365 nm for 15 min, the mixture was purified by precipitation in cold hexanes–methanol mixed solvent (v/v = 1/10) three times. The white solid was collected after filtration and dried in a vacuum oven at 25 °C for 24 h to afford the PS–(FPOSS)–PCL (47 mg, 75%) as a white powder. ^{1}H NMR ($CDCl_3$, 500 Hz, ppm, δ): 7.30–6.30 (m, 332H), 4.01 (m, 228H), 3.65 (t, 2H, -CH_2OH), 2.90–2.60 (m, 28H), 2.36 (m, 230H), 2.10–1.00 (m, 900H), 1.00–0.55 (m, 10H), 0.35–0.15 (m, 6H). ^{13}C NMR ($CDCl_3$, 125 Hz, ppm, δ): shown in Fig. S3d†. FT-IR (KBr) ν (cm^{-1}): 2941, 2867, 1729 (very strong), 1457, 1367, 1240, 1186, 1106, 1043, 756, 701. $M_{n,NMR}$ = 24.0 kg mol^{-1}. SEC: $M_{n,SEC}$ = 14.4 kg mol^{-1}, M_w/M_n = 1.16.

Results and discussion

General aspects of FPOSS-based shape amphiphiles

The importance of fluoro-containing compounds can never be underestimated in materials science. The introduction of fluoro-containing nano-building blocks can greatly expand the scope of shape amphiphiles while the presence of multiple interactions with different characteristic dominating length scales could benefit the construction of novel hierarchical structures. In designing such FPOSS-based shape amphiphiles, synthetic facility is the very first consideration. Highly fluorinated hybrid compounds are often difficult to prepare due to the incompatibility between fluorous materials and other functional materials, especially for simultaneously multi-site functionalization.[21] This can be circumvented by the use of "click" chemistry. Thiol–ene chemistry is now a well-established "click" process for various functionalizations and has been applied to the synthesis of a Janus particle based on perfluorinated POSS.[18] It has been found that thiol–ene "click" chemistry can effectively couple perfluorinated tails onto vinyl groups. Hence, vinyl groups can be used as chemical masks for potential site-specific incorporation of perfluorinated chains. Multiple-vinyl-functionalized POSS, such as OVPOSS and those shown in Schemes 1 and 2, are thus ideal precursors for FPOSS in the final materials. The advantage is that it eliminates many complications associated with fluorinated compounds and only introduces the perfluorinated chains at the last stage. Therefore, following a "growing-from" and "post-click-functionalization" method as we recently reported,[7] a FPOSS-based shape amphiphile can be readily made (Scheme 1). Additional functionalization on the POSS prior to "post-click functionalization" allows the construction of shape amphiphiles with more complex topologies and diverse compositions (Scheme 2). For example, as studied in mikto-arm copolymers by changing the number of tethering chains from 1 to 4 for a single junction point, the interfacial curvature is expected to change significantly.[34] Moreover, it is known that when the tethered chains contain different chemical compositions, they may become crystalline (*e.g.* PCL) or immiscible for phase-separation into various nanostructures (*e.g.* PS/PCL, or PS/PDMS). On the other hand, the composition of the FPOSS head could also be systematically varied, since fluorinated alkyl thiols with different fluoro-content can be used. In the current paper, 1*H*,1*H*,2*H*,2*H*-perfluoro-1-decanethiol was used since it is commercially available and gives a long perfluorinated tail. Overall, the strategy strives to fulfill the "click" philosophy to allow a modular, precise, and systematic control of important molecular parameters (*e.g.* molecular weight of each block, polydispersity, locations of functionality, *etc.*) for FPOSS-based shape amphiphiles.

FPOSS tethered with one homopolymer chain

The synthesis highlights a two-step, gram-scale preparation of FPOSS-based giant surfactants (Scheme 1). The hydroxyl group of VPOSS–OH[31] can initiate the ring opening polymerization (ROP) of ε-CL under the catalysis of $Sn(Oct)_2$, which is known to proceed in a controlled fashion with high functional group tolerance and yields PCL with narrow polydispersity and controlled molecular weight.[35] The polymerization was carried out in toluene with 0.5 equivalent of $Sn(Oct)_2$ at 65 °C to avoid possible side reactions. After a designed reaction time, the polymerization was quenched at a specific conversion and the polymer purification was achieved by repeated precipitation to remove excess monomer, which involves no fractionation and greatly facilitates the synthesis and scale-up. The VPOSS–PCL thus obtained possesses precisely defined structure with only one POSS per polymer chain. The presence of vinyl groups does not

interfere with the polymerization under the present reaction conditions. All the vinyl groups remain intact after polymerization, as shown by the peaks at δ 5.88–6.15 ppm in ^{1}H NMR spectrum (Fig. 1a). The uniformity and purity of the compound was evidenced by MALDI-TOF mass spectrum (Fig. 2a) and SEC trace (Fig. 3). In MALDI-TOF mass spectrum, only one single distribution could be observed with the *m*/*z* values [4323.3 Da for 32-mer, $C_{16}H_{25}O_{13}Si_8(C_6H_{10}O_2)_{32}H\cdot Na^+$] matching well with that of the calculated monoisotopic mass (4323.1 Da). The unimodal SEC trace appears to be symmetric and narrowly dispersed (PDI = 1.12). Compared to VPOSS–OH, the retention volume is also significantly shifted to a much lower value, indicating polymer formation and a large increase in molecular weight. The VPOSS–PCL can then be directly subject to further functionalization.

The fluorination was performed by reacting VPOSS–PCL with 1*H*,1*H*,2*H*,2*H*-perfluoro-1-decanethiol in the presence of DMPA under UV irradiation for 15 min. Repeated precipitation into a mixture of methanol and hexanes was necessary to remove the excess fluorinated thiols. The successful ligation was proven by the complete disappearance of POSS vinyl proton resonances at δ 5.88–6.15 ppm and the appearance of the two peaks from methylene linkages at δ 2.76–2.60 ppm in the ^{1}H NMR spectrum that can be attributed to the two methylene units near the thioether (Fig. 1b). Similarly, in the ^{13}C NMR spectrum (Fig. S1b†), no vinyl sp^2 carbons could be observed. The installment of seven fluorous chains significantly increases the molecular weight ($M_{w,\ FPOSS}$ = 4009.8 Da). In MALDI-TOF mass spectrum, the major molecular weight distribution completely shifts to a higher molecular weight region (Fig. 2b). Although isotopic resolution is not available at this molecular weight range, the observed average *m*/*z* (7683.8 Da) was in favorable agreement with the calculated one (7686.0 Da for 32-mer $[M_{32}\cdot Na]^+$, $C_{278}H_{381}F_{119}O_{77}S_7Si_8Na^+$). There is another minor distribution that is ~16 Da higher in molecular weight than the major distribution. This could be attributed to either the molecule with

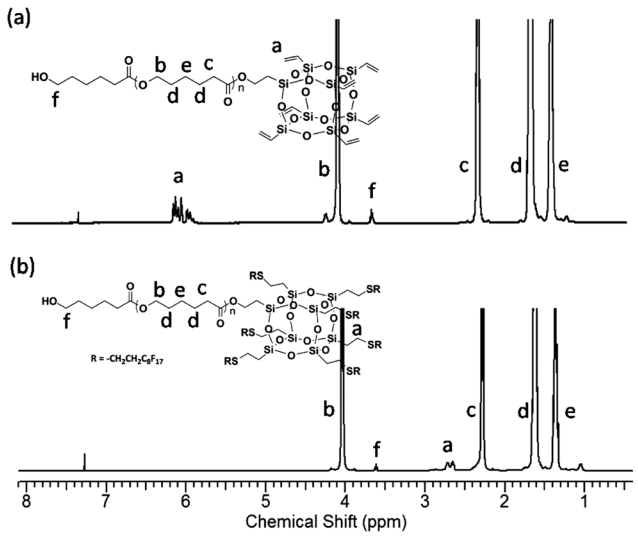

Fig. 1 ^{1}H NMR spectra of (a) VPOSS–PCL and (b) FPOSS–PCL. The complete disappearance of the vinyl protons at δ 5.88–6.15 ppm and the emergence of new characteristic resonances at δ 2.60–2.76 ppm indicate complete functionalization.

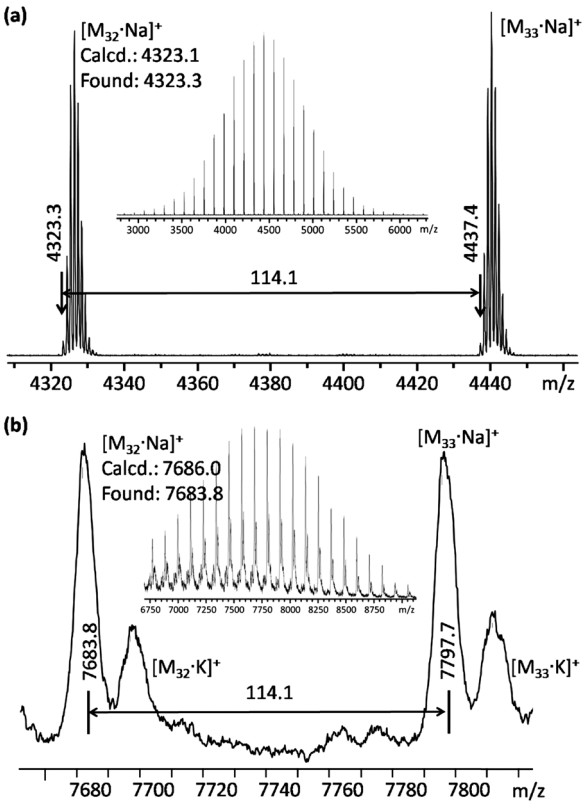

Fig. 2 MALDI-TOF mass spectra of (a) VPOSS–PCL and (b) FPOSS–PCL.

a potassium ion or the oxidized molecule with a sodium ion, which is commonly observed for thiol–ene products.[36] While the molecular weights obtained from SEC and ^{1}H NMR show reasonably good agreement, it is noteworthy that the average molecular weights observed from mass spectra in both VPOSS–PCL and FPOSS–PCL are apparently lower than those obtained from ^{1}H NMR spectra and SEC, which can be rationalized by the much lower ionization efficiency for high molecular weight

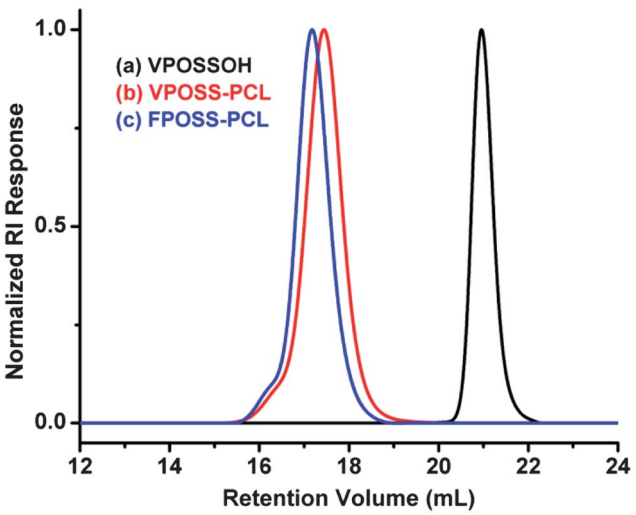

Fig. 3 SEC overlay of (a) VPOSS–OH (black), (b) VPOSS–PCL (red), and (c) FPOSS–PCL (blue).

fractions (Table 1).[37] The SEC trace also shows a slight shift to lower retention volume due to molecular weight increase but it remains narrow. Meanwhile, it was found that the reaction often generates some high molecular weight shoulders as seen by the small bump on the SEC trace. Similar observations have been reported previously in literature for thiol–ene process, especially for relatively large and bulky thiols, and have been attributed to radical recombination to form dimers.[7] Care should be taken to minimize these side reactions by performing the reaction with a larger excess of thiols. Nevertheless, the chemical structure and homogeneity of the fluorous giant surfactant are unambiguous.

FPOSS tethered with two compositionally distinct polymer chains

Synthesis of ditethered FPOSS-based shape amphiphiles requires a ω-chain-end hetero-functionalized polymer precursor. Previously in our work, we have demonstrated a hydrosilyl-functionalized diphenylethylene derivative (DPE-SiH) as a versatile intermediate for the preparation of various in-chain-functionalized polymers and hetero-functionalized polymers using living anionic polymerization.[32] Using this approach as previously reported, the precursor, PS–(SiH)–OH, was prepared in a single one-pot process by reacting poly(styryl)lithium with DPE-SiH to giving a living polymer followed by quantitative end-capping with ethylene oxide and quenching with degassed methanol. The product has been thoroughly characterized by FT-IR (Fig. S4a†), ^{1}H NMR (Fig. 4a), ^{13}C NMR (Fig. S3a†), and MALDI-TOF MS (Fig. 5a) and was found to possess $M_{n,SEC}$ of 6.9 kg mol^{-1} and a narrow PDI of 1.02. While the hydroxyl group is known to be versatile for various chemical transformations, the Si–H bond was recently found to be a favorable combination with anionic polymerization due to the following characteristics: (1) it is compatible with the highly reactive anionic chain-ends and thus requires no protection/deprotection step; (2) the hydrosilyl-capped polystyrene can be prepared in large quantities and stored over long periods of time in the presence of air and moisture; (3) it becomes very reactive towards various alkenes in the presence of catalysts; and (4) the reaction is effective and tolerant to a variety of functional groups.[32,38] Therefore, hydrosilylation has been proposed to be a general functionalization methodology for anionic polymers and has been used to synthesize many polymer architectures.[37,38] In this case, PS–(SiH)–OH was reacted with commercially available OVPOSS to prepare VPOSS-end-capped PS–(VPOSS)–OH. This is similar to the "grafting-to" coupling approach. Due to the presence of multiple vinyl groups, such reaction is usually concomitant with the formation of higher addition products where fractionation is often necessary.[6] However, due to the presence of hydroxyl group which affects the overall polarity of the mono-tethered and di-tethered product, simple silica gel chromatography using toluene as eluent (R_f = 0.50–0.55) was sufficient to separate the mono-functionalized PS–(VPOSS)–OH in a moderate yield of

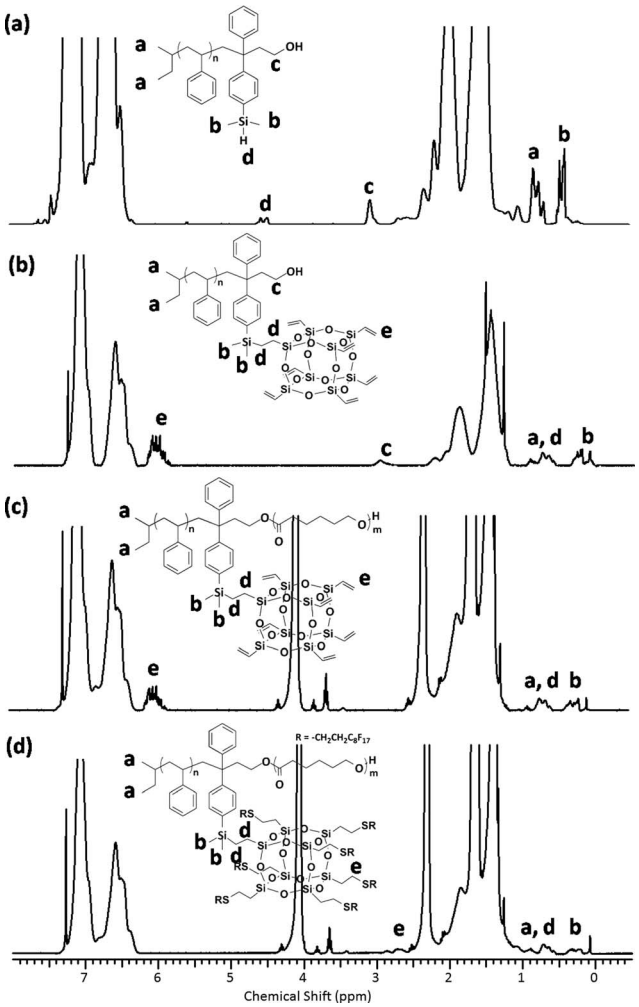

Fig. 4 ^{1}H NMR spectra of (a) PS–(SiH)–OH, (b) PS–(VPOSS)–OH, (c) PS–(VPOSS)–PCL, and (d) PS–(FPOSS)–PCL.

Table 1 Summary of molecular characterizations

Sample	$M_{n,SEC}$ (g mol^{-1})	$M_{n,NMR}$ (g mol^{-1})			$M_{n,MALDI}$ (Da)	$M_{n,Calcd.}$ (Da)	PDI
		XPOSS	PS	PCL			
VPOSS–PCL	8.1k	650	—	6.7k	4323.3[a]	4323.1[a]	1.12
FPOSS–PCL	9.6k	4009.8	—	6.7k	7683.8[b]	7686.0[b]	1.10
PS–(SiH)–OH	6.9k	—	6.9k	—	6070.7[c]	6070.7[c]	1.02
PS–(VPOSS)–OH	7.7k	650	6.9k	—	6719.5[d]	6718.6[d]	1.01
PS–(VPOSS)–PCL	12.9k	650	6.9k	13.7k	—	—	1.04
PS–(FPOSS)–PCL	14.4k	4009.8	6.9k	13.7k	—	—	1.16

[a] Monoisotopic molecular mass based on 32-mer with sodium ion. [b] Average molecular mass based on 32-mer with sodium ion. [c] Monoisotopic molecular weight based on 55-mer with lithium ion. [d] Monoisotopic molecular weight based on 55-mer with sodium ion.

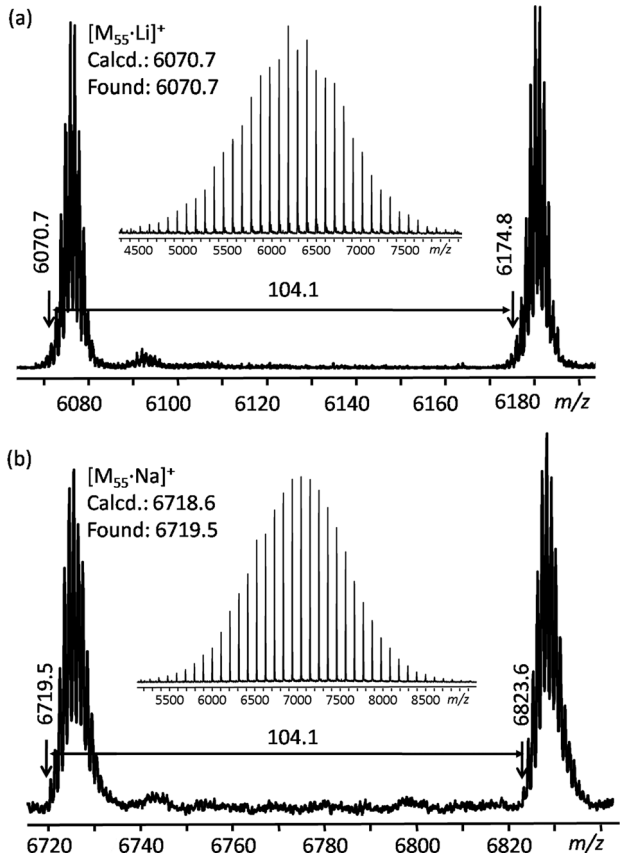

Fig. 5 MALDI-TOF mass spectra of (a) PS–(SiH)–OH and (b) PS–(VPOSS)–OH showing one major distribution corresponding to the desired structure.

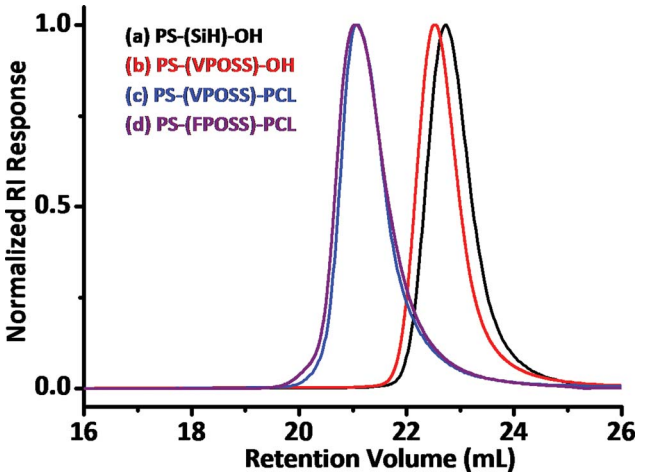

Fig. 6 SEC trace overlay of (a) PS–(SiH)–OH (black), (b) PS–(VPOSS)–OH (red), (c) PS–(VPOSS)–PCL (blue), and (d) PS–(FPOSS)–PCL (purple).

~44%. The addition of a POSS nanoparticle is evident from the SEC spectrum in Fig. 6 by the slight shift to lower elution volume and a slight increase of molecular weight to 7.7 kg mol^{-1}. The molecular weight distribution was still narrow (PDI = 1.01) and no high molecular weight shoulders could be observed. From the FT-IR spectrum (Fig. S4b†), the absorption at 2115 cm^{-1} ascribed to the Si–H stretching vibration was completely disappeared while the new band at around 1120 cm^{-1} is characteristic of the Si–O–Si asymmetric stretching in the POSS cage. Fig. 4b shows the ^{1}H NMR spectrum of PS–(VPOSS)–OH where one can find that the peak at about δ 4.50 ppm (Si–H) was completely disappeared and the new peaks appear at δ 5.90–6.20 ppm, which are characteristic of the vinyl protons on POSS cage. The new vinyl carbons can also be seen at δ 136.8 ppm in ^{13}C NMR spectrum (Fig. S3b†). In the MALDI-TOF mass spectrum (Fig. 5b), a single narrow distribution can be clearly seen and the observed molecular weight agreeing well with the calculated one of the proposed structure. A representative monoisotopic mass peak at *m*/*z* 6719.5, which corresponds to the 55-mer of PS–(VPOSS)–OH–Na^{+}, $C_4H_9(C_8H_8)_{55}C_{34}H_{47}Si_9O_{13}Na^{+}$, is in good agreement with the calculated monoisotopic mass (6718.6 Da). These results indicate that only one POSS cage with seven vinyl groups was attached on the polymer chain-end and there is an additional hydroxyl group ready for further functionalization. Following the same route as in the previous section, the macroinitiator, PS–(VPOSS)–OH, can be used to prepare PS–(FPOSS)–PCL in a sequential chain growth and "click" functionalization process.

The hydroxyl-initiated ring opening polymerization of ε-CL using the PS–(VPOSS)–OH macroinitiator was performed at 65 °C for 24 hours and the polymer was purified by repeated precipitation. The block copolymerization was first demonstrated by SEC trace (Fig. 6) which shows a symmetric, monomodal peak with a molecular weight of 12.9 kg mol^{-1} and a narrow polydispersity (PDI = 1.04) and was completely shifted to lower retention volume with baseline resolution as compared to the precursor PS–(VPOSS)–OH. In this series of samples, it was found that the molecular weights given by SEC (either by light scattering or PS standard calibration) were significantly lower than that calculated from ^{1}H NMR spectra. To cross-prove the accuracy of the molecular weight measurements, the samples were tested in two different SEC instruments. However, in both cases similar results were obtained (Table S1†). It was speculated that the unique composition and architecture of the shape amphiphiles are the source of discrepancy between the results from SEC and those from the ^{1}H NMR spectra. By tethering a conformationally rigid nanoparticle in between two blocks, the overall conformation of the shape amphiphile in solution might not be fully expanded due to the congested geometry at the junction point, resulting in a more compact random coil and thus an apparently lower molecular weight. Nevertheless, the integrity of PCL block is clearly shown by the strong characteristic carbonyl stretching vibration at 1729 cm^{-1} in the FT-IR spectrum (Fig. S4c†). Meanwhile, all those protons or carbons assignable to methylene units on PCL backbone can be clearly seen and unambiguously assigned.[39] Moreover, the VPOSS cage remains intact during the polymerization, which is affirmed by the peaks of vinyl protons at δ 6.20–5.90 ppm in the ^{1}H NMR spectrum (Fig. 4c) and at δ 136.7 ppm for vinyl carbons in ^{13}C NMR spectrum (Fig. S3c†). Although we were unable to perform MALDI-TOF mass analysis for this sample due to its high molecular weight and complex chemical composition, the current evidence strongly supports the chemical structure as proposed.

The final fluorination of the POSS cage was performed using the same reaction condition as in the preparation of FPOSS–PCL. Successful functionalization was achieved in less than 15 minutes and was affirmed by the complete disappearance of vinyl proton resonances on POSS cage at δ 6.20–5.90 ppm and the new appearance of two peaks at δ 2.90–2.60 ppm in ^{1}H NMR spectrum (Fig. 4d), which are ascribed to vinyl protons and the methylene groups of the thiol ether linkage, respectively. However, the signals from the methylene protons near -CF_2 group could not be clearly distinguished in the ^{1}H NMR spectrum because they overlapped with the peaks from protons on the PS block backbone. Similarly, in the ^{13}C NMR spectrum (Fig. S3d†), although the new peaks attributed to the carbons of perfluorinated alkyl chains on POSS could hardly be seen, they are probably significantly suppressed by the very strong signal from the PCL backbone. In addition, no vinyl carbons could be observed, which again suggests complete functionalization. All the chemical shifts could be clearly assigned and were in good agreement with those of the reported analogues.[18] In SEC overlay (Fig. 6), the installation of seven fluorous chains does not seem to change dramatically the hydrodynamic volume of the polymer. The molecular weight given by SEC increases only slightly from 12.9 kg mol^{-1} for PS–(VPOSS)–PCL to 14.4 kg mol^{-1} for PS–(FPOSS)–PCL. Again, the molecular weight given by SEC for these di-tethered FPOSS shape amphiphiles is significantly lower than that calculated from ^{1}H NMR. As discussed above, this is probably because of the unique architecture of the shape amphiphile with a functional POSS nanoparticle at the junction point. It is also anticipated that since FPOSS is tethered at the junction point of the diblock copolymer, the fluorination does not alter the overall hydrodynamic volume very much. In addition, the huge difference in chemical composition between FPOSS and the PS standards used to calibrate SEC might contribute large error to the measurements. Although MALDI-TOF mass analysis is unavailable, all of the aforementioned evidence strongly supports the formation of PS–(FPOSS)–PCL as proposed. It is also anticipated that different kinds of functional groups can be conveniently introduced onto POSS to prepare various XPOSS-based shape amphiphiles.

Conclusions

In summary, we have reported the design and synthesis of two shape amphiphiles based on fluorinated polyhedral oligomeric silsesquioxane (FPOSS). In the two examples provided here, FPOSS was either tethered to the end of a PCL chain or to the junction point of a PS-*b*-PCL block copolymer. The combination of living anionic polymerization and the "growing-from" strategy of ring-opening polymerization together with the highly efficient thiol–ene "click" reaction resulted in the successful incorporation of FPOSS into various polymeric scaffolds. The products were fully characterized by ^{1}H NMR, ^{13}C NMR, FT-IR, MALDI-TOF mass spectrometry, and SEC. This study has established FPOSS as a versatile nano-sized fluorous particle building block in hybrid materials and the shape amphiphiles presented in this work serve as model compounds to reveal the versatility of this method and to explore their self-assembly behaviors, in which the interplay between bulk phase separation and crystallization are expected to create rich phase behavior and intriguing hierarchical structures. The studies on their self-assembly and phase behaviors are currently ongoing in our laboratory and will be discussed in future publications.

Acknowledgements

This work was supported by NSF (DMR-090689) and the Joint-Hope Education Foundation. We thank Dr Xiaopeng Li and Prof. Chrys Wesdemiotis for help with the MALDI-TOF mass spectrometry. J. H. acknowledges the financial support from China Scholarship Council and the Innovative Graduate Education Program of Jiangsu Province (CX09B_021Z).

Notes and references

1 R. W. Date and D. W. Bruce, *J. Am. Chem. Soc.*, 2003, **125**, 9012–9013.
2 S. C. Glotzer, M. A. Horsch, C. R. Iacovella, Z. Zhang, E. R. Chan and X. Zhang, *Curr. Opin. Colloid Interface Sci.*, 2005, **10**, 287–295.
3 S. C. Glotzer and M. J. Solomon, *Nat. Mater.*, 2007, **6**, 557–562.
4 X. Zhang, E. R. Chan and S. C. Glotzer, *J. Chem. Phys.*, 2005, **123**, 184718.
5 Z. L. Zhang, M. A. Horsch, M. H. Lamm and S. C. Glotzer, *Nano Lett.*, 2003, **3**, 1341–1346.
6 X. Yu, S. Zhong, X. Li, Y. Tu, S. Yang, R. M. Van Horn, C. Ni, D. J. Pochan, R. P. Quirk, C. Wesdemiotis, W.-B. Zhang and S. Z. D. Cheng, *J. Am. Chem. Soc.*, 2010, **132**, 16741–16744.
7 W.-B. Zhang, Y. Li, X. Li, X. Dong, X. Yu, C.-L. Wang, C. Wesdemiotis, R. P. Quirk and S. Z. D. Cheng, *Macromolecules*, 2011, **44**, 2589–2596.
8 Y. W. Jun, J. W. Seo, S. J. Oh and J. Cheon, *Coord. Chem. Rev.*, 2005, **249**, 1766–1775.
9 V. Kitaev, *J. Mater. Chem.*, 2008, **18**, 4745–4749.
10 A. J. Patil and S. Mann, *J. Mater. Chem.*, 2008, **18**, 4605–4615.
11 N. F. Steinmetz, A. Bize, K. C. Findlay, G. P. Lomonossoff, M. Manchester, D. J. Evans and D. Prangishvili, *Adv. Funct. Mater.*, 2008, **18**, 3478–3486.
12 I. C. Reynhout, J. J. L. M. Cornelissen and R. J. M. Nolte, *Acc. Chem. Res.*, 2009, **42**, 681–692.
13 S. Sun, C. B. Murray, D. Weller, L. Folks and A. Moser, *Science*, 2000, **287**, 1989–1992.
14 G. R. Newkome, C. N. Moorefield and F. Vögtle, *Dendritic Macromolecules: Concepts, Syntheses, Perspectives*, Wiley-VCH, New York, 1997.
15 G. Kickelbick, *Prog. Polym. Sci.*, 2003, **28**, 83–114.
16 D. Cordes, P. Lickiss and F. Rataboul, *Chem. Rev.*, 2010, **110**, 2081–2173.
17 K. Prassides and H. Alloul, *Fullerene-Based Materials: Structures and Properties*, Springer, Berlin; New York, 2004.
18 Y. Li, W.-B. Zhang, I.-F. Hsieh, G. Zhang, Y. Cao, X. Li, C. Wesdemiotis, B. Lotz, H. Xiong and S. Z. D. Cheng, *J. Am. Chem. Soc.*, 2011, **133**, 10712–10715.
19 H.-J. Sun, Y. Tu, C.-L. Wang, R. M. Van Horn, C.-C. Tsai, M. J. Graham, B. Sun, B. Lotz, W.-B. Zhang and S. Z. D. Cheng, *J. Mater. Chem.*, 2011, **21**, 14240–14247.
20 X. Ren, B. Sun, C.-C. Tsai, Y. Tu, S. Leng, K. Li, Z. Kang, R. M. V. Horn, X. Li, M. Zhu, C. Wesdemiotis, W.-B. Zhang and S. Z. D. Cheng, *J. Phys. Chem. B*, 2010, **114**, 4802–4810.
21 E. de Wolf, G. van Koten and B.-J. Deelman, *Chem. Soc. Rev.*, 1999, **28**, 37–41.
22 W. Zhang, *Chem. Rev.*, 2009, **109**, 749–795.
23 J. Mabry, A. Vij, S. Iacono and B. Viers, *Angew. Chem., Int. Ed.*, 2008, **47**, 4137–4177.
24 T. Homma, K. Harano, H. Isobe and E. Nakamura, *Angew. Chem., Int. Ed.*, 2010, **49**, 1665–1668.
25 M. Meldal and C. W. Tornoe, *Chem. Rev.*, 2008, **108**, 2952–3015.
26 W. Zhang and A. H. E. Muller, *Macromolecules*, 2010, **43**, 3148–3152.
27 C. E. Hoyle and C. N. Bowman, *Angew. Chem., Int. Ed.*, 2010, **49**, 1540–1573.

28 M. J. Kade, D. J. Burke and C. J. Hawker, *J. Polym. Sci., Part A: Polym. Chem.*, 2010, **48**, 743–750.
29 H. Gilman and F. K. Cartledge, *J. Organomet. Chem.*, 1964, **2**, 447–454.
30 N. Hadjichristidis, H. Iatrou, S. Pispas and M. Pitsikalis, *J. Polym. Sci., Part A: Polym. Chem.*, 2000, **38**, 3211–3234.
31 F. J. Feher, K. D. Wyndham, R. K. Baldwin, D. Soulivong, J. D. Lichtenhan and J. W. Ziller, *Chem. Commun.*, 1999, 1289–1290.
32 W.-B. Zhang, B. Sun, H. Li, X. Ren, J. Janoski, S. Sahoo, D. E. Dabney, C. Wesdemiotis, R. P. Quirk and S. Z. D. Cheng, *Macromolecules*, 2009, **42**, 7258–7262.
33 K. Gunes, A. I. Isayev, X. P. Li and C. Wesdemiotis, *Polymer*, 2010, **51**, 1071–1081.
34 G. M. Grason and R. D. Kamien, *Macromolecules*, 2004, **37**, 7371–7380.
35 C. Jérôme and P. Lecomte, *Adv. Drug Delivery Rev.*, 2008, **60**, 1056–1076.
36 J. W. Chan, C. E. Hoyle and A. B. Lowe, *J. Am. Chem. Soc.*, 2009, **131**, 5751–5753.
37 J. Liu, R. S. Loewe and R. D. McCullough, *Macromolecules*, 1999, **32**, 5777–5785.
38 Y. Li, W.-B. Zhang, J. E. Janoski, X. Li, X. Dong, C. Wesdemiotis, R. P. Quirk and S. Z. D. Cheng, *Macromolecules*, 2011, **44**, 3328–3337.
39 W.-B. Zhang, J. He, X. Dong, C.-L. Wang, H. Li, F. Teng, X. Li, C. Wesdemiotis, R. P. Quirk and S. Z. D. Cheng, *Polymer*, 2011, **52**, 4221–4226.

